Materials Research. 2017; 20(2): 339-348
DOI: http://dx.doi.org/10.1590/1980-5373-MR-2016-0544

Effects of Methylcellulose on the Properties and Morphology of Polysulfone Membranes Prepared by Phase Inversion

Meriem Nadour[a]*, Fatima Boukraa[a], Adel Ouradi[a,b], Ahmed Benaboura[a]

[a]Laboratoire Synthèse Macromoléculaire et Thioorganique Macromoléculaire, Faculté de Chimie, Université des Sciences et de la Technologie Houari Boumediene, USTHB, B.P 32 El-Alia, Algiers, Algeria
[b]Faculté des Sciences, Université Saad Dahleb de Blida, route Soumaa, BP 270, Blida, Algeria

Received: July 18, 2016; Revised: October 31, 2016; Accepted: December 17, 2016

Polymer solutions of polysulfone (PSf) and methylcellulose (MC) in 1-methyl-2-pyrrolidone (NMP) were used to prepare ultrafiltration membranes by the phase inversion technique via immersion precipitation. The effect of MC additive on the structure and performances of the membranes was studied. The obtained membranes were characterized by scanning electron microscopy (SEM), differential scanning calorimetry (DSC), infrared spectroscopy (FTIR-ATR), equilibrium water content (EWC), water contact angle, porosity and ultrafiltration experiments of polyethylene glycol solutions. It was found that all the PSf/MC membranes had higher porosity, more hydrophilic surface and more vertically finger like pores than PSf membrane. With an increase in MC content in the casting solution from 0.5% to 1.5%, the hydraulic permeability increases from 17.17 to 118.46 $L.m^{-2}.h^{-1}.bar^{-1}$, while the rejection decreases from 91.82% to 64.45% with PEG 35000. DSC scan and FTIR analysis confirmed that methylcellulose was trapped in the membranes matrix.

Keywords: *Polymeric membrane, Polysulfone, Methylcellulose polymer.*

1. Introduction

Most materials such as polymer, ceramic, metal, carbon and glass can be used to make membranes[1,2]. At present, the commercial membranes are mainly fabricated from polymeric materials. Being membrane materials, the polymers should demonstrate thermal stability over a wide range of temperature and a chemical stability over a range of pH, and possess a strong mechanical strength. The polymers that are suitable for making membranes include cellulose acetate[3,4], polyamides[5,6], polysulfones[7,8], sulfonated polysulfones[9,10], etc.. Polysulfones are mainly used to form ultrafiltration, microfiltration and gas separation membranes. They are also used to form the porous support layer of many reverse osmosis, nanofiltration and some gas separation membranes.[11-13]

Polysulfone is one of the most used polymers to prepare membranes due to its excellent characteristics such as high chemical, thermal and mechanical resistance. However, polysulfone membranes exhibit strong adsorption and deposition towards foulants on the membrane surface as well as inside membrane pores due to the hydrophobic nature of polysulfone. This results in a lower water flux and serious membrane fouling. Hence, polysulfone membranes without modification seem less suitable for application in industry[14,15]. In order to improve membrane permeability and anti-fouling behavior, several studies have been devoted to this subject. Among these approaches, polymeric additives[15,16] are considered as an effective and convenient method because of their excellent performance and facility to handle. Polyvinylpyrrolidone [17-19], poly (ethylene glycol) [20-22] and the polyaniline (emeraldine base) [14] were used as additives in the preparation of polysulfone membranes to promote their performances. Such additives act as a porogen which favors the formation of pores, also as agent for hydrophilizing the membranes surface. Most of these studies reported that the polymeric additives enhance the membrane surface hydrophilicity, water permeability and improved membrane fouling resistance characteristics.

According to the literature, the synthetic polymeric additives have been used extensively in membrane preparation in order to improve their separation properties, while natural plant-based polymers are rarely reported in this field. Among these polymers, the methylcellulose is classified as an amphiphilic natural plant-based polymer[23] and can be used as an additive to prepare membranes[24]. A new membrane prepared from modified methylcellulose/ cellulose acetate mixture was used to separate the emulsion oil in water[25]. Gcina et al.[26] used a lignin as an additive to probe the mechanical and thermal properties of polysulfone membranes. The result is the formation of thermally stable membranes relative to membranes modified with polyethylene glycol and polyvinyl pyrrolidone. Besides, they concluded that lignin is a good additive due to its interaction with the polymer through hydrogen bonding and make it a reinforcing agent. Therefore, the use of natural additives, cheap and readily available can be a good choice for membranes preparation.

* e-mail: nadourmeriem@gmail.com

In this study, flat sheet membranes were prepared using a cellulose derivative polymer, methylcellulose, as an additive *via* phase inversion method, in order to create a high performance material that is based on renewable resources. The effect of methylcellulose as an additive on the properties of polysulfone membranes was evaluated using infrared spectroscopy, thermal analysis, electron microscopy, pure water flux and solute rejection studies.

2. Experimental

2.1. Materials

Polysulfone (PSf, Udel P-3500, M_w: 35000 Da) used as membrane material was supplied by Solvay Advanced Polymer (Belgium). Methylcellulose (MC, Mn~63000 Da, vis.1500 cps) from Aldrich was used as an additive. The molecular formulas of theses polymers are represented in Figure 1. N-methyl-2-pyrrolidone (NMP, 99%) from Fluka was used as solvent directly without any further purification. Polyethylene glycols of different molecular weights (6000, 10000 and 35000 Da) from Fluka were used to measure the rejection and molecular weight cut-off of the membranes. Bismuth (III) nitrate pentahydrate ($BiN_3O_9.5H_2O$), potassium iodide (KI) and hydrochloric acid (HCl) were analytical reagents provided by Sigma-Aldrich factory used to prepare Dragendorff reagent.

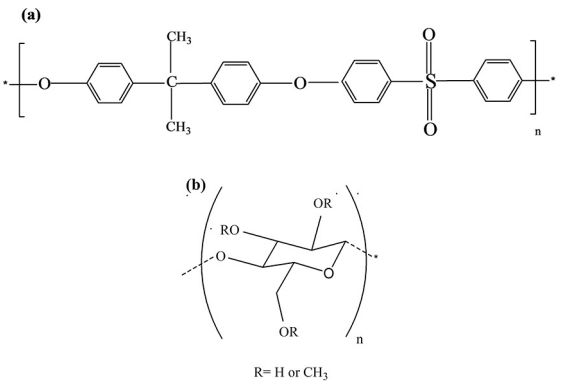

Figure 1: The molecular formulas: (a) polysulfone and (b) methylcellulose.

2.2. Membrane preparation

Flat sheet polysulfone-based membranes were prepared by phase inversion method *via* immersion precipitation in water coagulation bath as reported in literature[27-29]. Several polysulfone solutions were prepared by dissolving a measured amount of polymer (16 wt %) in NMP at room temperature. Then different quantities of methylcellulose were added in viscous polysulfone solutions, as shown in table 1. The polymeric mixture was stirred using a magnetic stirrer until having a homogeneous solution (~24h), and then it was left without stirring for 30 minutes to remove air bubbles. Thereafter, the solution was spread uniformly on a glass plate into ca.300 µm film with the help of a casting knife. The resulting film was then immersed directly into coagulation bath containing water maintained at fixed temperature (25°C). The casted films changed their color from transparent to white immediately after immersion and separates out of the glass plate after a few seconds. The prepared membranes were stored in distilled water until use.

Table 1: The compositions of the PSf/MC/NMP casting solutions.

Membranes	Composition of casting solution (wt %)		
	PSf	MC	NMP
PSf	16.0	0	84.0
PSf-0.5	16.0	0.5	83.5
PSf-1	16.0	1.0	83.0
PSf-1.5	16.0	1.5	82.5

2.3. Technical characterization

2.3.1. Thermogravimetric analysis (TGA)

The degradation property of methylcellulose polymer was determined using thermogravimetric analyzer (TGA Instrument Q500). The sample of pure methylcellulose was used without preparation and it was heated from 30 °C to 575 °C at a heating rate of 10 °C.min^{-1} under nitrogen atmosphere.

2.3.2. Differential scanning calorimetry (DSC)

The thermal behavior of the methylcellulose and of the prepared membranes was investigated by differential scanning calorimetry (Jade DSC instrument, Perkin Elmer), to measure the glass transition temperatures (Tg). For each measurement 5-8 mg of samples were weighed and scanned, from 25 to 250 °C, under dry nitrogen.

2.3.3. Chemical analysis

The powdered sample of methylcellulose and the membranes surface were analyzed by a Fourier transform infrared spectroscopic method with attenuated total reflectance (Perkin Elmer- Spectrum Two spectrophotometer) between 450 and 4000 cm^{-1} at a resolution of 2 cm^{-1} with 32 scans. Before analysis, the membranes were dried in an oven at 50 °C to remove water traces.

2.3.4. Membrane morphology

The cross section morphologies of the membranes were observed by an electron microscope (SEM) (Philips ESEMXL 30). Before SEM analysis, the membrane samples were cut into appropriate size, frozen in liquid nitrogen and fractured.

2.3.5. Contact angle (CA)

In order to evaluate the hydrophilic / hydrophobic character of membranes, water contact angles were measured

using a measuring instrument (GBX DIGIDROP "Digitizer of droplets"). A drop of water (1µl) was deposited on the membrane surface using a syringe. When the droplet is formed on the surface, an image of the drop was taken using a video camera. To minimize experimental error, the contact angle was measured at three different locations for each sample and the average was then reported.

2.4. Membrane characterization by the determination of equilibrium water content (EWC) and porosity

Equilibrium water content is a parameter related to porosity and can predict the degree of hydrophilicity or hydrophobicity of a membrane [30].

2.4.1. Equilibrium Water content (EWC)

The membrane samples were cut in the dimension of 3×3 cm and put in distilled water for 24 hours, then weighed after removing excess of water on the surface. After that, the membrane samples were dried in an oven at a temperature of 50 °C until a constant mass was obtained (~24h). The equilibrium water content is calculated as follows:

$$\mathrm{EWC}\,(\%) = \frac{W_W - W_d}{W_W} \times 100 \quad (1)$$

Where W_w and W_d are the mass of the wet membrane sample and the mass of the dried state (g) respectively.

To minimize the error, three pieces of each membrane were cut.

2.4.2. Membrane porosity

The membrane porosity was obtained by Eq.2.[31]

$$\mathrm{P}\,(\%) = \frac{W_W - W_d}{\rho \times A \times L} \times 100 \quad (2)$$

Where W_w and W_d are the mass of the wet membrane sample and the mass of the dried state (g) respectively. A, L and ρ are the sample area (cm^2), the sample thickness (cm) at wet state and pure water density (g/cm^3) respectively.

2.5. Hydrodynamic characterization

Filtration experiments were performed using a dead end filtration stirred cell (Model 8050, 50ml, Amicon) connected to a nitrogen pressure. Each fresh membrane was compacted before use. The compaction was carried out with deionized water for 30 minutes at 1 bar. The pure water flux was measured in a range of pressure of 0.6 to 4 bars. For each membrane, several discs were tested and the average pure water flux was reported.

2.5.1. Pure water flux (PWF)

The pure water flux was calculated using Eq. (3)

$$\mathrm{J} = \frac{V}{A \times \Delta t} \quad (3)$$

Where J ($L.m^{-2}.h^{-1}$) is the pure water flux, V (L) is the volume of filtrate, A (m^2) is the membrane area and Δt (h) is the filtration time.

Hydraulic permeability (P_h) was obtained from the slope of the plot of J and ΔP and was calculated using Eq.4 [32]

$$\mathrm{P}_h = \frac{J}{\Delta P} \quad (4)$$

2.5.2. Solute rejection (SR)

The rejection rate of the membranes was determined by filtration of PEG solutions of different molecular weights at a pressure of 1 bar. The solute rejection was calculated using Eq. (5)

$$\mathrm{SR} = (1 - \frac{C_p}{C_f}) \times 100 \quad (5)$$

Where C_p and C_f are the concentrations of permeate and feed solutions respectively, which were determined by Dragendorff reagent method using spectrophotometry analysis.[33]

3. Results and Discussion

3.1. DSC and FTIR Characterization of membranes

During the immersion/ precipitation of casting solution, on the one hand, the water soluble methylcellulose is extracted by the coagulant (water) in order to make porous polysulfone membrane with absence of MC. On the other hand, the coagulated chains of polysulfone surround the MC chains and bloc them in the matrix due to the instantaneous demixing of polymers solution. Consequently, the extraction of all the amount of MC from the polymer film cannot easily occur due to the short time of the coagulation.

In this aim, the thermal behavior and chemical surface analysis are studied in order to prove the presence of MC on the membrane matrix.

3.1.1. Differential Scanning Calorimetry (DSC)

Prior to differential thermal analysis (DSC), the thermal degradation by TGA studies of such a sample is needed. A TGA analysis was performed for MC to determine its temprature degradation.

The TGA thermogram of MC (figure 2) shows one decomposition stage and a minor weight loss of 4% at around 100 °C due to moisture and water retention from the polysaccharide structure. The decomposition process observed for this sample starts at 300 °C and shows only one max differential thermo-gravimetric (DTG) peak at 358.70 °C, indicates a good thermal stability of the methylcellulose used. These results are similar to those reported in the literature by Guimes et al.[34] and Zohuriaan et al.[35]

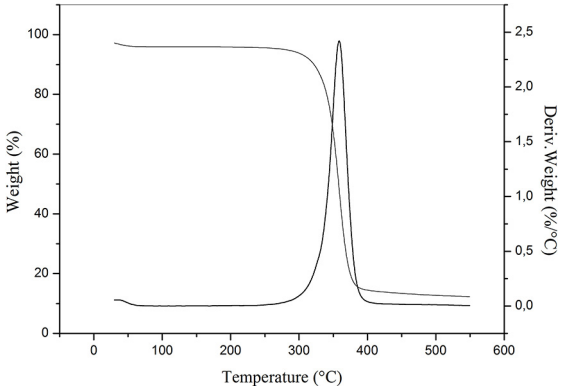

Figure 2: TGA thermogram of methylcellulose.

From the DSC thermogram of methylcellulose (Figure 3), it can be seen that the water flow endotherm occurs in the range of 80 °C and 100 °C. This endotherm is present on the thermograms of cellulosic materials due to the interaction of the water and the non-substituted hydroxyl groups of the cellulose derivatives[36]. The presence of an endotherm at 147 °C in DSC can be attributed to a glass transition, as reported in literature[37]. Zuo et al. found a glass transition temperature of a commercial MC (M450) of about 108.7 °C.

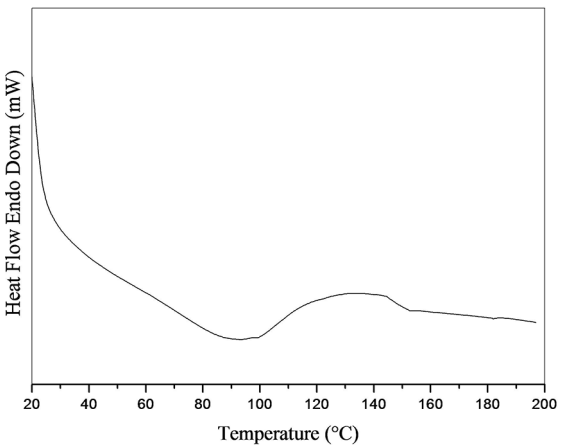

Figure 3: DSC thermogram of methylcellulose.

The thermal behaviors of different membranes were studied from DSC plots. Figure 4 presents the DSC results of the prepared membranes. From the above spectra, only a single glass transition temperature is observed in the range of 180-200 °C for all the membranes. The thermograme of control membrane (PSf) shows a glass transition temperature at 189.39 °C. The thermogrames of PSf/MC membranes show glass transition temperatures at 182.19 °C, 185.17 °C and 184.38 °C respectively by increasing the amount of methylcellulose in the polymer mixture from 0.5% to 1.5%. Comparing to the controle membrane, the Tg of PSf/MC membranes is slightly lower, this may be due to the presence of flexible side groups (Alkyl) of MC that increase the distance between chains in the mixture and reduces the inter-chain interactions that cause a decrease in Tg[28]. Generally, a lower glass transition temperature indicates more free volume in polymer which tends to release its molecular structure[26].

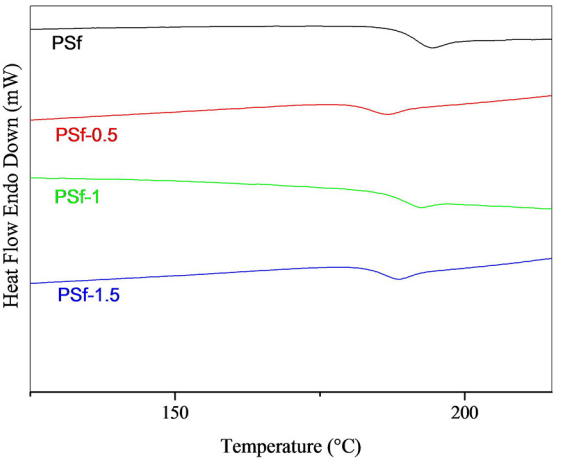

Figure 4: DSC thermograms of the membranes.

The slight changes of Tgs in DSC curves reflect the small amounts of MC in membranes. Consequently, the thermal properties of these membranes are near to those of control membrane.

3.1.2. Membrane surface chemistry

The functional groups present in the control membrane, in the methylcellulose and in the PSf/MC membranes were obtained by attenuated total reflection Fourier transform infrared spectroscopy (FTIR-ATR), and the recorded spectra are shown in Figures 5, 6 and 7 respectively.

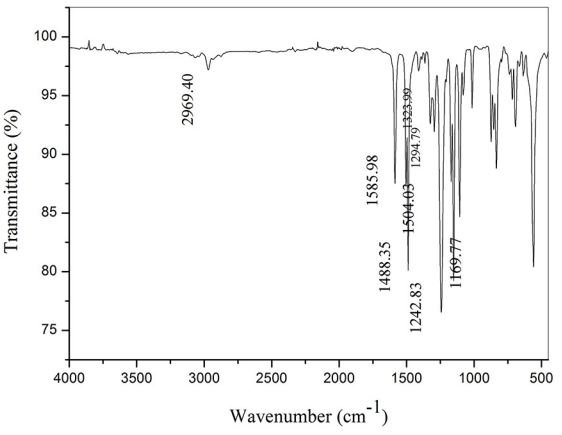

Figure 5: The FTIR-ATR spectra of the control membrane.

The FTIR spectrum of the control membrane (Figure 5) displayed the characteristics absorption peaks of all the bonds, in which the absorption band at 2969.40 cm^{-1} is attributed to C-H stretching vibrations. The presence of a strong peak

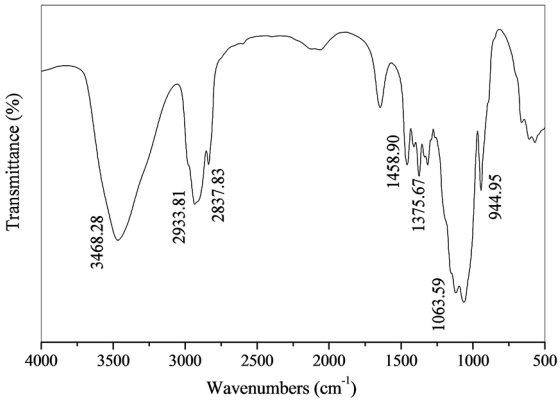

Figure 6: The FTIR-ATR spectra of pure methylcellulose.

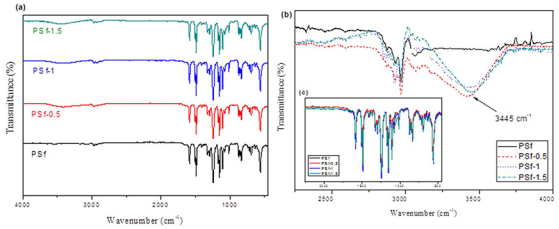

(a) 4000-450 cm^{-1} (b) 4000-2250 cm^{-1}

Figure 7: The FTIR-ATR spectra of the membranes: (a) 4000-450 cm^{-1}, (b) 4000-2250 cm^{-1} et (c) 2250-450 cm^{-1}.

at 1242.83 cm^{-1} is assigned to the ether C-O-C stretch of the polysulfone moiety. The aromatic carbon carbon (C=C) streching vibration occurs at 1585.98 cm^{-1}, 1504.03 cm^{-1} and 1488.35 cm^{-1}. The peaks at 1323.99 cm^{-1},1294.79 cm^{-1} and 1169.77 cm^{-1} correspond to a symmetric stretch of the sulfone group (SO_2), and these results are consistent with previous works.[14,38]

The FTIR-ATR spectroscopy was used to examine the functional groups of methylcellulose. The FTIR-ATR spectrum of MC (Figure 6) shows that pure methylcellulose had an absorption band at 3468.28 cm^{-1} related to stretching vibration of hydroxyl group ν(O-H). The bands at 2933.81cm^{-1}, 2837.83 cm^{-1} are attributed to asymmetric and symmetric stretching vibration of C-H respectively. The pics at 1375.67 and 1458.9 cm^{-1} are assigned to the vibration of deformation in the plane of δ(C-H). The absorption band at 1063.59 cm^{-1} is ascribed to C-O-C stretching mode from glucosidic units. The peak at 944.95 cm^{-1} is related to OCH_3 groups. These results were consistent with those reported in the literature.[39,40]

All peaks infrared absorption characteristics of PSf are present in FTIR spectra of PSf/MC membranes (Figure 7a,7c). In addition to the PSf absorption peaks, new peaks were observed in the region of 3200-3500 cm^{-1} characteristic to the hydroxyl groups (O-H) due probably to the presence of MC in the membranes matrix (Figure 7b).

3.2. Membrane morphology

The structure of the membrane is affected by the composition of the casting solution, where the nature and concentration of additives play important roles in the modification of the membrane properties. To evaluate the morphology of the membranes, the cross-sections of different prepared ultrafiltration membranes were characterized by SEM images and presented in figures 8 and 9. It can be seen that the membranes exhibit an asymmetric structure with a dense skin in the top layer and open pores (macrovoids and finger like pores) at the sublayer (Figure 8)

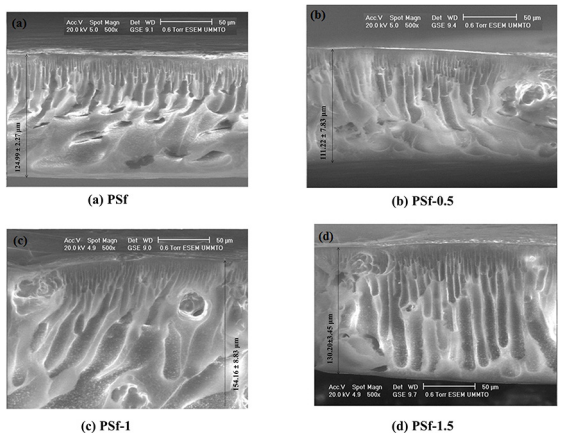

Figure 8: Cross-section SEM images of the prepared membranes (magnification ×500): (a) PSf, (b) PSf-0.5, (c) PSf-1 and (d) PSf-1.5.

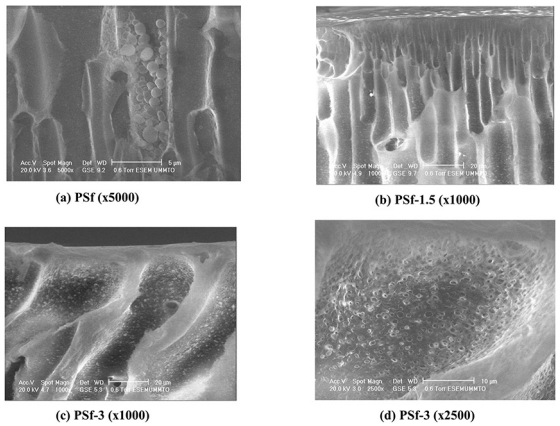

Figure 9: SEM images of the prepared membranes showing the honeycomb-cell morphology: (a) PSf (×5000), (b) PSf-1.5 (×1000), (c) PSf-3 (×1000) and (d) PSf-3 (×2500).

The cross-sectional morphology of the control membrane display both finger like pores and macrovoids near the bottom. This structure is formed by an instantaneous demixing produced between the surface of polymer casting solution and water coagulation bath[30,41] which results a formation of polymer reach phase and poor phase.

In fact, the instantaneous demixion of membrane is due to (1) the incompatibility of the system PSf/ water results the precipitation of PSf and (2) the high mutual affinity between the solvent (NMP) and the non-solvent (water) results the high diffusion between solvent and non-solvent at the interface of casting solution. Consequently,

the polymer-reach phase produces the thin film and the formation of nuclei of a polymer-poor phase form the porous structure [42]. The formation of finger like pores in sub-layer is the result of a longer exchange between solvent and non-solvent in polymer poor phase follows the increase of solution viscosity which cause a delayed precipitation of the polymer and then, a decrease in the diffusion rate of water into the polymer film [43,44].

Compared with the control membrane, the finger like pores and macrovoids of PSf/MC membranes become more porous with increasing concentrations of MC. A similar observation was found by Gcina et al.[26] for the PSf membrane using ligning as an additive and NMP as a solvent. Generaly, water soluble polymers have been considered as pore-formers during membrane formation [45]. It is assumed that most of water soluble polymers can be leached out of the casting film and the sites where the polymer exists become micropores in the prepared membrane[14]. The evolutions found in cross-section confirm that the water soluble methylcellulose form pores when used, as additive, in membranes. In fact, the MC has good solubility in NMP, a portion of MC located near the surface of the casting film could diffuse out along with NMP into the coagulation bath, resulting in the increase of membrane porosity.

At higher magnification, a spongy morphology appeared between the open pores with the PSf/MC membranes as shown in Figures 9b. For a clear observation of this morphology, membrane at 3% of MC was prepared and analysed by SEM (Figures 9c and d).

For the controle membrane, the fast formation of the rigid PSf matrix prevents the growth of the polymer-lean droplets (spongy structure) in between the macrovoids [46,47]. It is well known that the structure of the membrane is affected by the kinetic diffusion of solvent and non solvent. In our system PSf/ NMP/water, the high affinity between water and NMP induce the instantaneous demixion and form asymetric membrane. In the contrary case, the low affinity between solvent/non solvent induce the delayed demixion and the spongious structure become favorable. The open pores structure in controle membrane are formed by nucleation and growth of the polymer lean phase due to the formation of skin layer. The early formation of skin layer delay the diffusion of water through the top layer which cause the delayed demixion of sublayer. This new phenomenon is not produced from the lower affinity of solvent/ non solvent but produced by the low concentration of non solvent in polymer poor phase. In this region, the solvent concentrations become so high locally, these conditions become favorable for delay of demixing [48]. In this case, a nucleus is formed serving as a tiny coagulation bath. The polymer solution surrounding the nucleus. As long as the conditions of delayed demixing remain the same, as long as the solvent concentration in the nucleus remains high enough, the growth of the nucleus continues [48].

However, the spongious structure in between open pores was observed in controle membrane at hight concentration of PSf [49]. Gillen et al. explain that the polymer precipitation also occurs rapidly at the inner walls of the finger like voids and forms a thin skin and the region between open pores remain fluid. The slow diffusion of non-solvent into the inter-void regions of the membrane causes nucleation of the polymer rich phase and eventually polymer precipitation, hence a spongy morphology arises from precipitated nuclei.

With the PSf/ MC/ NMP/water system, the integrated hydrophilic polymer MC in skin layer make the diffusion of water through the top layer relatively higher compared with the controle membrane. The conditions for delay of demixing cannot take place in some points: growth of a nucleus is effectively blocked by the creation of new nuclei. Such structure is observed by SEM microscopy for the PSf/ AN69/NMP systems[47], when the non water soluble polymer (AN69) was used as an additive. The longer time is observed before the matrix vitrification which allows the nucleated polymer-lean droplets to grow further in the delayed phase-separation zones, leading to larger cells in the spongy part between the open pores.

3.3. Equilibrium water content, porosity and hydrophilicity

All the prepared membranes were characterized in terms of equilibrium water content (EWC), porosity and surface hydrophilicity. The results are presented in table 2. The EWC is considered as a parameter that indirectly indicates the degree of hydrophilicity of a membrane and it is closely related to the porosity. The pores on the surface as well as cavities in the sublayer are responsible for accommodating water in the membranes[30,32]. It may be found from the table that a small increase in EWC is observed with increasing the rate of MC in membranes, and the values are around 74-75%. This indicates the increment of the number of pores in the membrane or the pore size of the existing pores.

A significant increase in porosity is found when MC content increases in polymer solutions. The PSf/MC membranes showed a high porosity in the range of 68% to 81% compared to the control membrane that present a porosity of 57%. This may be the results of hydrophilic character of MC which lead to form the spongy structure between the open pores.

Water contact angle is a parameter used to evaluate the surface hydrophilicity and also one of the most important parameter which could affect the flux of the membranes. As presented in table 2, the contact angle of the PSf /MC membranes is lower than that of the control membrane and decreases by 2° when increasing the concentration of MC by 0.5%. The variation in the contact angle is small; it reflects a small change in the hydrophilic nature of the membrane surface which can be explained by the low rate of

Table 2: Membranes characteristics.

Membranes	EWC (%)	Contact angle (°) (s.d)*	Porosity (%)	P_h ($L.m^{-2}.h^{-1}.bar^{-1}$)	MWCO
PSf	74.40	66.01 (3.68)	57.64	4.71	-
PSf-0.5	74.66	64.58 (4.33)	68.70	17.17	35000
PSf-1	74.82	62.16 (0.87)	75.05	28.29	≈35000
PSf-1.5	75.54	60.30 (4.11)	81.40	118.46	>35000

* Standard deviation.

MC trapped in the membrane and/or the lack of hydrophilic group (hydroxyl) in the methylcellulose.

During the immersion precipitation process, the MC can diffuse on the membrane surface due to its good solubility in water, leading to the improvement of wettability on the membrane surface due to its hydrophilic groups (OH). Therefore, contact angle is closely related with surface energy [32].

3.4. Effects of MC on membrane permeability and solute rejection

Pure water flux (PWF) and solution rejection are considered to be significant factors for any membranes. PWF and solute rejection have a direct relationship with the number of pores and the pore size on the membrane surface. The effect of MC rate on PWF and solute rejection is shown in the Figures 10 and 11. It can be seen from Figure 10 that PWF increases with increasing in transmembrane pressure linearly. This result verifies Darcy's law, which means that in this case, the transport through a membrane is described by Darcy's law. The free volume elements (pores) are relatively large and fixed, do not fluctuate in position or volume on the timescale of permeant motion, and are connected to one another [2]. From the same figure, it can be observed that the membrane *which* contains 1.5% MC, exhibits the highest water flux of 45.31 $L.m^{-2}.h^{-1}$ and 427.40 $L.m^{-2}.h^{-1}$ at 0.6 bar and 4 bars respectively. The variation of the water flux could be explained by the porosity of the membranes. It is observed from table 2 that a significant increase in porosity is found when the amount of MC increased in a polymer solution.

From the same figure, it can be observed that the membrane permeability was improved by increasing the amount of MC in polymers solutions. The control membrane shows a low permeability of 4.71 $L.m^{-2}.h\text{-}1.bar^{-1}$, and then it was increses to 17.17, 28.29 and 118.46 $L.m^{-2}.h^{-1}.bar^{-1}$ respectively by increasing the MC content from 0.5 to 1.5%. These can be the results of the double effect of MC manifested by the improvement of membrane surface hydrophilicity (table 1) and the alteration of the membrane structure. The increase of MC content leads to a larger pores compared to the control membrane, so that the water molecules penetrate easily through the membrane.

Another term used to define the performance of membranes is the removal percentage of unwanted solute. Ultrafiltration membranes are porous membrane, wich indicate that the basic mechanism of rejection will be the sieving mechanism. Molecules with a greater size than the pores will be rejected. From the solute rejection results (Figure 11), the rejection of PEG 35000, PEG 10000 and PEG 6000 by the membranes are in the ranges of 64.45 - 91.82%, 31.57 - 82.30% and 21.43 - 70.77% respectively. For all the membranes, the rejections decrease with increasing MC content in a polymer solution in the following order PEG 35000 rejection >PEG 10000 rejection > PEG 6000 rejection. This is due to the difference of molecular weights. Consequently, the pore size of the PSf/MC membranes increases with the amount of MC, which is in complete agreement with the values of the permeability where hydraulic permeability increases from 17.17 to 118.46 $L.m^{-2}.h^{-1}.bar^{-1}$ by increasing the rate of MC from 0.5% to 1.5% (Table 2).

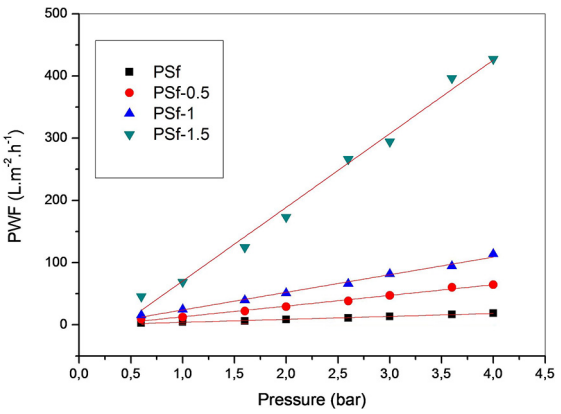

Figure 10: Effect of MC dosage on the pure water flux at different trans-membrane pressure (20°C, ΔP 0.6-4 bar).

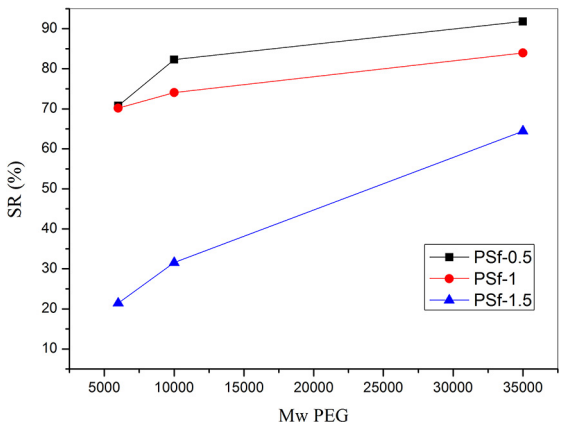

Figure 11: Effect of MC dosage on solute rejection of the membranes.

The molecular weight cut-off (MWCO) is defined as the lowest molecular weight of a solute that has a rejection of 90% [50]. According to this, the MWCO of the PSf/MC membranes is higher than 35000 Da for PSf-1.5, is about 35000 Da for PSf-1, and is 35000 Da for PSf-0.5.

4. Conclusion

In order to study the effect of methylcellulose as an additive on membrane structure and performances, polysulfone based membranes were prepared *via* phase inversion method and different amounts of methylcellulose were added to the polymer solution. The morphology of the modified membranes shows an asymmetric structure with a dense skin at the surface and both finger like pores and macrovoids penetrating the membrane cross section. At higher magnification, a spongy morphology was observed between finger like pores with the excepetion for the control membrane. On the one hand, the evolutions found in cross-section confirm that the water soluble methylcellulose could leach out in the coagulation bath during phase separation and act as pore forming agent, on the other hand, FTIR-ATR and DSC results demonstrate that a amount of MC remains trapped in the matrix of the prepared membranes. The increase in membrane porosity by increasing the amount of MC in polymer solutions enhance pure water flux and consequently decrease the PEG rejection, and the contact angle of different membranes show an improvement in the surface hydrophilicity.

The results obtained in this work suggest that the natural plant-based polymers may be promising additives in membrane formation and demonstrate a good performance; thus, it can be considered as an additive in practical applications.

It could be interesting to study the effect of different types of soluble cellulose derivatives in term of morphology, pore size and performance against the effluent treatment, and make a comparative study with those prepared with synthetic additives.

5. References

1. Wang LK, Chen JP, Hung YH, Shammas NK, eds. *Membrane and Desalination Technologies.* Handbook of Environmental Engineering. Volume 13. New York: Springer; 2011.

2. Baker RW. *Membrane Technology and Applications*. 2nd ed. Chichester: John Wiley & Sons; 2004.

3. Han B, Zhang D, Shao Z, Kong L, Lv S. Preparation and characterization of cellulose acetate/carboxymethyl cellulose acetate blend ultrafiltration membranes. *Desalination*. 2013;311:80-89.

4. Sabad-e-Gul, Waheed S, Ahmad A, Khan SM, Hussain M, Jamil T, Zuber M. Synthesis, characterization and permeation performance of cellulose acetate/polyethylene glycol-600 membranes loaded with silver particles for ultra-low pressure reverse osmosis. *Journal of the Taiwan Institute of Chemical Engineers*. 2015;57:129-138.

5. Poletto P, Duarte J, Thürmer MB, Santos V, Zeni M. Characterization of Polyamide 66 membranes prepared by phase inversion using formic acid and hydrochloric acid such as solvents. *Materials Research*. 2011;14(4):547-551.

6. Saeki D, Nagao S, Isao S, Ohmukai Y, Maruyama T, Matsuyama H. Development of antibacterial polyamide reverse osmosis membrane modified with a covalently immobilized enzyme. *Journal of Membrane Science*. 2013;428:403-409.

7. Sinha MK, Purkait MK. Increase in hydrophilicity of polysulfone membrane using polyethylene glycol methyl ether. *Journal of Membrane Science*. 2013;437:7-16.

8. Kumar S, Guria C, Mandal A. Synthesis, characterization and performance studies of polysulfone/bentonite nanoparticles mixed-matrix ultra-filtration membranes using oil field produced water. *Separation and Purification Technology*. 2015;150:145-158.

9. Padaki M, Isloor AM, Wanichapichart P, Ismail AF. Preparation and characterization of sulfonated polysulfone and N-phthloyl chitosan blend composite cation-exchange membrane for desalination. *Desalination*. 2012;298:42-48.

10. Chen SH, Liou RM, Lin YY, Lai CL, Lai JY. Preparation and characterizations of asymmetric sulfonated polysulfone membranes by wet phase inversion method. *European Polymer Journal*. 2009;45(4):1293-1301.

11. Zhao C, Xue J, Ran F, Sun S. Modification of polyethersulfone membranes - A review of methods. *Progress in Materials Science*. 2013;58(1):76-150.

12. Holda AK, Aernouts B, Sayes W, Vankelecom IFJ. Study of polymer concentration and evaporation time as phase inversion parameters for polysulfone-based SRNF membranes. *Journal of Membrane Science*. 2013;442:196-205.

13. Lee S, Lee JS, Lee M, Choi JW, Kim S, Lee S. Separation of sulfur hexafluoride (SF_6) from ternary gas mixtures using commercial polysulfone (PSf) hollow fiber membranes. *Journal of Membrane Science*. 2014;452:311-318.

14. Zhao S, Wang Z, Wei X, Zhao B, Wang J, Yang S, et al. Performance improvement of polysulfone ultrafiltration membrane using PANiEB as both pore forming agent and hydrophilic modifier. *Journal of Membrane Science*. 2011;385-386:251-262.

15. Mosqueda-Jimenez DB, Narbaitz RM, Matsuura T, Chowdhury G, Pleizier G, Santerre JP. Influence of processing conditions on the properties of ultrafiltration membranes. *Journal of Membrane Science*. 2004;231(1-2):209-224.

16. Chakrabarty B, Ghoshal AK, Purkait MK. Preparation, characterization and performance studies of polysulfone membranes using PVP as an additive. *Journal of Membrane Science*. 2008;315(1-2):36-47.

17. Susanto H, Ulbricht M. Characteristics, performance and stability of polyethersulfone ultrafiltration membranes prepared by phase separation method using different macromolecular additives. *Journal of Membrane Science*. 2009;327(1-2):125-135.

18. Myeong JH, Suk TN. Thermodynamic and rheological variation in polysulfone solution by PVP and its effect in the preparation of phase inversion membrane. *Journal of Membrane Science*. 2002;202:55-61.

19. Javiya S, Yogesh, Gupta S, Singh K, Bhattacharya A. Porometry Studies of the Polysulfone Membranes on Addition of Poly (ethylene Glycol) in Gelation Bath During Preparation. *Journal of the Mexican Chemical Society*. 2008;52(2):140-144.

20. Panda SR, De S. Preparation, characterization and performance of $ZnCl_2$ incorporated polysufone (PSF)/Polyethylene glycol (PEG) blend low pressure nanofiltration membranes. *Desalination*. 2014;347:52-65.

21. Holda A, Vankelecom IFJ. Integrally skinned PSf-based SRNF-membranes prepared via phase inversion—Part A: Influence of high molecular weight additives. *Journal of Membrane Science*. 2014;450:512-521.

22. Holda A, Vankelecom IFJ. Integrally skinned PSf-based SRNF-membranes prepared via phase inversion—Part B: Influence of low molecular weight additives. *Journal of Membrane Science*. 2014;450:499-511.

23. Wertz JL, Bédué O, Mercier JP. *Cellulose Science and Technology*. 1st ed. Lausanne: EPFL Press; 2010.

24. Kim JH, Lee KH. Effect of PEG additive on membrane formation by phase inversion. *Journal of Membrane Science*. 1998;138(2):153-163.

25. Barbar R, Durand A, Ehrhardt JJ, Fanni J, Parmentier M. Physicochemical characterization of a modified cellulose acetate membrane for the design of oil-in-water emulsion disruption devices. *Journal of Membrane Science*. 2008;310(1-2):446-454.

26. Vilakati GD, Hoek EMV, Mamba BB. Probing the mechanical and thermal properties of polysulfone membranes modified with synthetic and natural polymer additives. *Polymer Testing*. 2014;34:202-210.

27. Van de Witte P, Dijkstra PJ, van den Berg JWA, Feijen J. Phase separation processes in polymer solutions in relation to membrane formation. *Journal of Membrane Science*. 1996;117:1-31.

28. Mulder M. *Basic Principles of Membrane Technology*. 2nd Ed. Dordrecht: Kluwer Academic Publishers; 1996.

29. Saljoughi E, Amirilargani M, Mohammadi T. Effect of PEG additive and coagulation bath temperature on the morphology, permeability and thermal/chemical stability of asymmetric CA membranes. *Desalination*. 2010;262(1-3):72-78.

30. Chakrabarty B, Ghoshal AK, Purkait MK. Effect of molecular weight of PEG on membrane morphology and transport properties. *Journal of Membrane Science*. 2008;309(1-2):209-221.

31. Ma Y, Shi F, Ma J, Wu M, Zhang J, Gao C. Effect of PEG additive on the morphology and performance of polysulfone ultrafiltration membranes. *Desalination*. 2011;272(1-3):51-58.

32. Garcia-Ivars J, Alcaina-Miranda MI, Iborra-Clar MI, Mendoza-Roca JA, Pastor-Alcañiz L. Enhancement in hydrophilicity of different polymer phase-inversion ultrafiltration membranes by introducing PEG/Al_2O_3 nanoparticles. *Separation and Purification Technology*. 2014;128:45-57.

33. Jia Z, Tian C. Quantitative determination of polyethylene glycol with modified Dragendorff reagent method. *Desalination*. 2009;247(1-3):423-429.

34. Rodrigues Filho G, Assunção RMN, Vieira JG, Meireles CS, Cerqueira DA, Barud HS, et al. Characterization of methylcellulose produced from sugar cane bagasse cellulose: Crystallinity and thermal properties. *Polymer Degradation and Stability*. 2007;92(2):205-210.

35. Zohuriaan MJ, Shokrolahi F. Thermal studies on natural and modified gums. *Polymer Testing*. 2004;23(5):575-579.

36. Vieira RGP, Rodrigues Filho G, Assunção RMN, Meireles CS, Vieira JG, Oliveira GS. Synthesis and characterization of methylcellulose from sugar cane bagasse cellulose. *Carbohydrate Polymers*. 2007;67(2):182-189.

37. Zuo M, Song Y, Zheng Q. Preparation and properties of wheat gluten/methylcellulose binary blend film casting from aqueous ammonia: A comparison with compression molded composites. *Journal of Food Engineering*. 2009;91(3):415-422.

38. Rafizah WAW, Ismail AF. Effect of carbon molecular sieve sizing with poly(vinyl pyrrolidone) K-15 on carbon molecular sieve-polysulfone mixed matrix membrane. *Journal of Membrane Science*. 2008;307(1):53-61.

39. Rimdusit S, Somsaeng K, Kewsuwan P, Jubsilp C, Tiptipakorn S. Comparison of Gamma Radiation Crosslinking and Chemical Crosslinking on Properties of Methylcellulose Hydrogel. *Engineering Journal*. 2012;16(4):15-28.

40. Maity D, Mollick MM, Mondal D, Bhowmick B, Bain MK, Bankura K, et al. Synthesis of methylcellulose-silver nanocomposite and investigation of mechanical and antimicrobial properties. *Carbohydrate Polymers*. 2012;90(4):1818-1825.

41. Riyasudheen N, Sujith A. Formation behavior and performance studies of poly(ethylene-co-vinyl alcohol)/poly(vinyl pyrrolidone) blend membranes prepared by non-solvent induced phase inversion method. *Desalination*. 2012;294:17-24.

42. Saljoughi E, Mousavi SM. Preparation and characterization of novel polysulfone nanofiltration membranes for removal of cadmium from contaminated water. *Separation and Purification Technology*. 2012;90:22-30.

43. Garcia-Ivars J, Iborra-Clar MI, Alcaina-Miranda MI, van der Bruggen B. Comparison between hydrophilic and hydrophobic metal nanoparticles on the phase separation phenomena during formation of asymmetric polyethersulphone membranes. *Journal of Membrane Science*. 2015;493:709-722.

44. Lin J, Ye W, Zhong K, Shen J, Jullok N, Sotto A, et al. Enhancement of polyethersulfone (PES) membrane doped by monodisperse Stöber silica for water treatment. *Chemical Engineering and Processing*. 2016;107:194-205.

45. Zhao S, Wang Z, Wei X, Tian X, Wang T, Yang S, et al. Comparison study of the effect of PVP and PANI nanofibers additives on membrane formation mechanism, structure and performance. *Journal of Membrane Science*. 2011;385-386:110-122.

46. Strathmann H, Kock K. The formation mechanism of phase inversion membranes. *Desalination*. 1977;21(3):241-255.

47. Ouradi A, Nguyen QT, Benaboura A. Polysulfone-AN69 blend membranes and its surface modification by polyelectrolyte-

layer deposit—Preparation and characterization. *Journal of Membrane Science*. 2014;454:20-35.

48. Boom RM, Wienk IM, van den Boomgaard T, Smolders CA. Microstructures in phase inversion membranes. Part 2. The role of a polymeric additive. *Journal of Membrane Science*. 1992;73(2-3):277-292.

49. Guillen GR, Ramon GZ, Pirouz Kavehpour H, Kaner RB, Hoek EMV. Direct microscopic observation of membrane formation by nonsolvent induced phase separation. *Journal of Membrane Science*. 2013;431:212-220.

50. Mohanty K, Purkait MK, eds. *Membrane Technologies and Applications*. Boca Raton: CRC Press; 2012.